Journal of
Analytical & Bioanalytical Techniques

Alsudir and Lai, J Anal Bioanal Tech 2015, 6:3
DOI: 10.4172/2155-9872.1000242

Research Article Open Access

Hydroxypropyl Methacrylate Interaction and Chitosan Coating for Enhanced UV Detection Sensitivity of Colloidal Nanoparticles in Capillary Electrophoresis Analysis

Samar Alsudir and Edward PC Lai*

Department of Chemistry, Ottawa-Carleton Chemistry Institute,Carleton University, Ottawa, ON K1S 5B6, Canada

Abstract

The binding interactions between silica (SiO_2), titania (TiO_2) or polymeric nanoparticles with hydroxypropyl methacrylate (HPMA) were investigated for enhancing the ultraviolet (UV) detection sensitivity of these nanoparticles in capillary electrophoresis (CE) analysis. HPMA interacted with colloidal SiO_2 nanoparticles, producing a larger CE-UV peak at a slightly shorter migration time. An increase in particle size with HPMA binding was validated using dynamic light scattering. The interaction was selective as HPMA did not interact with TiO_2 nanoparticles in aqueous suspension. Chitosan coating of SiO_2 or TiO_2 nanoparticles produced significantly larger hydrodynamic diameters to further enhance the sensitivity of their UV detection. The analytical technique, which involves coating SiO_2 nanoparticles with chitosan first and binding with HPMA next, is novel. It has allowed us to achieve a significant enhancement of 50 folds in detection sensitivity.

Keywords: Capillary electrophoresis; Chitosan; Colloid; Dynamic light scattering; Hydroxypropyl methacrylate; Nanoparticles; Polymer; Silica; Titania

Introduction

The growing use of inorganic oxide nanoparticles (NPs) [1-3], due to their novel properties and high biochemical reactivity [4], has led to unintended release of significant amounts of these NPs into the water cycle through industrial and household wastewater effluents [5-7]. The removal of NPs from water effluents varies in efficiency from 70% to 94% [8]. Their toxicity, especially to humans [9-11], arises from a number of biophysicochemical factors including their aggregation, chemical composition, concentration, dissolution, exposure routes, particle size, nanostructure, quantum effects, and self-assembly [12,13]. Uncertainties on their persistence in the water cycle have raised many concerns and provide the impetus to develop analytical techniques with high sensitivity to detect and quantify these NPs. Contemporary NPs quantification methods (such as laser induced break down detection [14], small angle neutron scattering [15], and fluorescent correlation spectroscopy [16] rely upon sophisticated instrumentation and a skilled analyst, making such approaches impractical for regular environmental monitoring.

Different chemistry-based encapsulation processes have been developed and showed promising results [17]. The growth of NPs in solution is complicated by several factors including changes in pH as well as interactions with ions and surfactants [18]. Either covalent attachment of end-functionalized polymers to the surface or in situ polymerization of monomers using immobilized initiator seems to be versatile [19] and [20]. Our novel approach is based on the controlled coating of NPs with a thick layer of polymer to grow them into a larger size for strong UV light absorption. The polymer coating also helps with the stabilization of NPs in aqueous suspension. These grown NPs can be separated by capillary electrophoresis (CE) due to differences in electrophoretic mobility, depending on their electronic charge, size, and surface functionality. A first coating of silica (SiO_2) NPs with polyhydroxypropyl methacrylate (PHPMA) was successfully developed in our laboratory to enhance the ultraviolet (UV) detection sensitivity by 6 folds during CE analysis [21]. A second coating with polydopamine (PDA) produced an extra 2-fold increase of the UV detection sensitivity to attain a total enhancement of 12 folds in detection sensitivity.

The goal of this study was to explore other coating materials that could further improve the CE-UV detection sensitivity for inorganic oxide nanoparticles (SiO_2 and TiO_2) in aqueous suspension. Investigation started with the binding interaction between these nanoparticles and HPMA, followed by coating with chitosan to produce larger diameters for enhanced UV detection sensitivities. Their hydrodynamic diameters were measured by dynamic light scattering and their ionic charge states were determined by capillary electrophoresis.

Material and Methods

Instrumentation

CE-UV analyses were performed on a laboratory built system, which includes a Spellman CZE1000R high-voltage power supply (Hauppauge, New York, USA). Fused-silica capillary (51 mm i.d., 356 mm o.d.) was obtained from Polymicro Technologies (Phoenix, AZ, USA). The background electrolyte (BGE) was composed of 10 mM Na_2HPO_4 in deionized distilled water (DDW) to attain pH 7.5 ± 0.2. Electrokinetic injection at 17 kV for 1.2 s, 3 s or 12 s was employed to load the sample into the capillary for CE analysis. All CE analyses were run at an applied voltage of 20 kV. A Bischoff Lambda 1010 (Leonberg, Germany) UV detector was set at a wavelength of 190 nm to determine the migration times of nanoparticles. A PeakSimple chromatography

***Corresponding authors:** Edward PC Lai, Ottawa-Carleton Chemistry Institute,Carleton University, Ottawa, ON K1S 5B6, Canada, Tel: +613-520-2600, Fax: +613-520-3749; Email: edward.lai@carleton.ca

Received April 08, 2015; **Accepted** April 28, 2015; **Published** May 05, 2015

Citation: Alsudir S, Lai EPC (2015) Hydroxypropyl Methacrylate Interaction and Chitosan Coating for Enhanced UV Detection Sensitivity of Colloidal Nanoparticles in Capillary Electrophoresis Analysis. J Anal Bioanal Tech 6: 242 doi:10.4172/2155-9872.1000242

data system (SRI model 203, Torrance, CA, USA) was used to acquire the detector output signal. The separated chemical compounds and/or nanoparticles were recorded in the electropherogram as peaks (represented by a blue line) with different migration times. Their peak areas above the baseline (represented by a pink line) were determined using a numerical integration algorithm.

The average diameters of SiO_2, TiO_2 and polymeric nanoparticles, before and after HPMA-binding or chitosan-coating, were measured by dynamic light scattering (DLS) using a Brookhaven Instruments nanoDLS particle size analyzer (Holtsville, NY, USA). Ten replicate measurements of 10 s each were performed to ensure high accuracy.

Reagents and materials

Chitosan (medium molecular weight of 190,000-310,000, deacetylation degree of 75-85%), 2-hydroxypropyl methacrylate (HPMA, 97%), mesityl oxide (MO, ≥ 90%), sodium dodecyl sulfate (SDS, ≥ 99%), LUDOX® colloidal silica (SiO_2, 30% wt suspension in H_2O, with a surface area of 198-250 m^2/g) and titanium oxide nanopowder (TiO_2, 21 nm) were all obtained from Sigma-Aldrich (Oakville, ON, Canada). 2,2′-azobis-2-isobutyronitrile (AIBN) was bought from Pfaltz & Bauer (Waterbury, CT, USA).

HPMA binding interaction with colloidal SiO_2 or TiO_2 nanoparticles

To investigate the binding interaction between HPMA and colloidal SiO_2 or TiO_2 nanoparticles, HPMA (3 ml) was first dissolved in DDW (25 ml) containing colloidal SiO2 or TiO_2 nanoparticles (20 mg/ml). Next, SDS (1.7 wt% of HPMA) was added and then the mixture was sonicated for 5 min to ensure homogeneity. Finally, the vial was placed in a 60C thermostatted water bath for 22 h to facilitate the binding interaction between HPMA and colloidal SiO_2 or TiO_2 nanoparticles. Percent binding of HPMA to SiO_2 or TiO_2 NPs was calculated as [(HPMA peak area before binding – HPMA peak area after binding)/HPMA peak area before binding] × 100% [22].

HPMA binding interaction with polymeric nanoparticles

A suspension of chitosan (1 wt%) in 1% acetic acid was prepared following a procedure reported by Shuai et al. [23]. The mixture was stirred magnetically for 3 h to obtain a homogeneous suspension. Then the chitosan suspension (1 ml) was added to 10 mM Na_2HPO_4 BGE (30 ml) containing colloidal SiO_2 or TiO_2 nanoparticles at varying concentrations (0-20 g/L), followed by magnetic stirring for 22 h. Addition of SDS (0.06 g) helped disperse the chitosan-coated particles to prevent precipitation. After addition of HPMA (0.03%, 0.05% or 0.1% v/v) to the chitosan-coated particles, the vial was placed in a 60°C thermostatted water bath for 22 h under continuous magnetic stirring.

Results and Discussion

CE-UV characterization of silica and titania nanoparticles

Growing interest in the development of nanocomposites consisting of TiO_2 and SiO_2 NPs has led to the release of these NPs in significant amounts to the water cycle, threating both humans and aquatic ecosystems. Cytotoxicity arises from the oxidative damage of these NPs owing to the production of reactive oxygen species. Moreover, TiO_2 NPs can further damage cells due to photocatalysis-enhanced oxidation upon exposure to light or UV radiation. Wastewater treatment plants and filters are often poorly suited to efficiently remove these NPs [24]. LUDOX® AM colloidal SiO_2 nanoparticles [25] do not settle and cannot be separated out by ordinary filtering or centrifuging like those in a suspension. In our work, an aliquot was spiked into the BGE that was loaded into the capillary by electrokinetic injection for CE-UV analysis. As shown in Figure 1a, 20 g/L of SiO_2 NPs exhibited low UV absorbance at the detection wavelength of 190 nm, producing a small peak at the migration time of 8.7 ± 0.1 min. The SiO_2 NPs appeared after the neutral marker, indicating their negative ionic charges (probably as SiO_4^{2-}) in the BGE and hence yielding a negative electrophoretic mobility value.

On the contrary, 20 g/L of TiO_2 NPs showed high UV absorbance at 190 nm, producing a large peak at the migration time of 8.4 ± 0.1 min, as shown in Figure 1b. Similar to SiO_2, TiO_2 NPs migrated after the neutral marker, which indicates their negative ionic charges in the BGE and therefore yielding a negative electrophoretic mobility value.

HPMA binding interaction with silica and titania nanoparticles

Binding interaction of HPMA with SiO_2 NPs was conducted at 60°C for 22 hours. The resultant SiO_2-HPMA particles were analyzed by CE-UV to determine their electrophoretic mobility. As shown in Figure 2, a new peak for HPMA-bound SiO_2 particles was detected at a migration time of 8.2 ± 0.1 min. These particles exhibited larger peak height and peak area than the original SiO_2 NPs (Figure 1a). Apparently, the SiO_2 NPs bound to HPMA to have their Si-O- groups buried under the surface, thus resulting in faster migration than SiO_2 NPs (at 8.7 ± 0.1 min) with good separation from HPMA (at 4.0 ± 0.1 min). HPMA binding to SiO_2 NPs was determined to be 19 ± 3%. Binding interaction of HPMA with TiO_2 NPs was next conducted at 60°C for

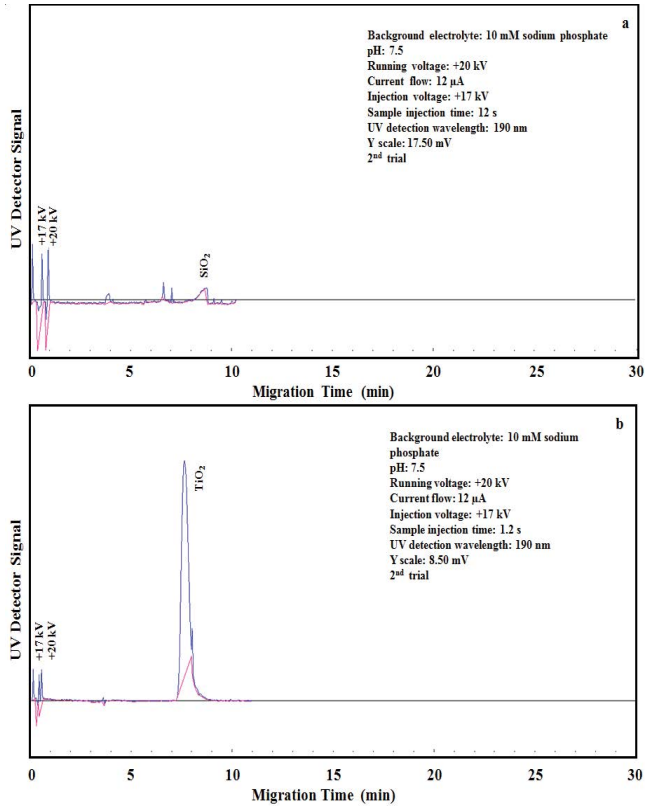

Figure 1: CE-UV characterization of (a) SiO_2 (20 g/L) and (b) TiO_2 (20 g/L) nanoparticles. SDS was present at a concentration of 2 mg/ml.

22 hours. CE-UV analysis of the mixture showed no sign of interaction between HPMA and TiO_2 NPs as no significant change was observed for the TiO_2 peak shape or its migration time. Correspondingly, HPMA binding to TiO_2 NPs was determined to be 0 ± 5 %. The oxygen atom of HPMA carbonyl group could interact with the Si atom of SiO_2 but not with the Ti atom of TiO_2. The difference between their interactions was likely due to the chemical properties of SiO_2 and TiO_2 NPs. Inorganic chemistry is highly dependent on the element; Si is a semiconductor and Ti is a metal.

Dynamic light scattering analysis of silica and titania nanoparticles

SiO_2 and TiO_2 NPs in aqueous suspension, as well as their mixtures with HPMA, were analyzed by DLS to determine their hydrodynamic diameters. In DLS analysis, multiple scattering (where light scattered from one particle is scattered from a second particle before reaching the detector) occurs to give the size distribution as particles undergo Brownian motion caused by thermally induced collisions between the suspended particles and solvent molecules. As shown in Figures 3a and 3b, the mean diameters of 53 ± 3 nm and 83 ± 13 nm were obtained for SiO_2 NPs and HPMA-bound SiO_2 particles, respectively. These results provide strong evidence that SiO_2 NPs became larger in size after interaction with HPMA under very simple experimental conditions. The interaction offers more sensitive detection of SiO_2 NPs (now in the form of HPMA-bound SiO_2 particles) by CE-UV, with optional electrophoretic separation from organic compounds possibly found in water. Mean diameters of 155 ± 6 nm and 154 ± 5 nm were obtained for TiO_2 NPs and their mixture with HPMA, respectively. DLS analysis confirmed that no interaction between TiO_2 NPs and HPMA took place as no significant change in the hydrodynamic diameter was observed.

Selectivity of HPMA binding with SiO_2 and TiO_2 nanoparticles

HPMA selectively interacted with colloidal SiO_2 NPs to produce a larger CE-UV peak at a slightly shorter migration time. It did not interact with TiO_2 NPs in aqueous suspension, resulting in no change of CE-UV peak area or migration time. This chemical method could allow us to analyze an aqueous sample containing the two kinds of nanoparticles, simply by adding HPMA and repeating the CE-UV analysis to observe any peak changes. A sample injection time of 3 s was used to maximize the resolution between different kinds of nanoparticles. Initially, SiO_2 NPs (20 g/L) produced a small peak (at 9.4 ± 0.1 min) with substantial overlap with the TiO_2 NPs (1 g/L) peak

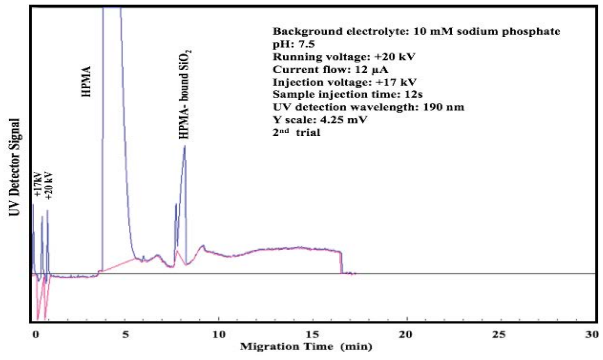

Figure 2: CE-UV characterization of SiO_2 (20 g/L) nanoparticles with 3.0 ml of HPMA. SDS was present at a concentration of 2 mg/ml.

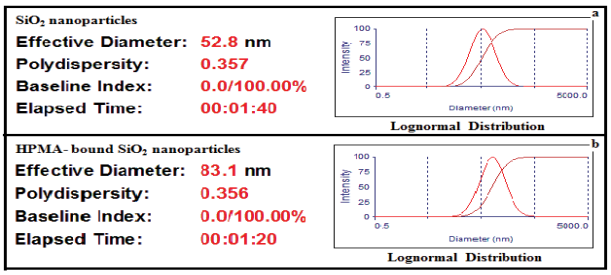

Figure 3: Dynamic light scattering measurements to determine the lognormal distribution of (a) SiO_2 nanoparticles and (b) HPMA-bound SiO_2 nanoparticles.

(at 8.6 ± 0.1 min). After 3 ml of HPMA were added, the HPMA-bound SiO_2 NPs moved ahead to appear as a sharp peak (at 8.4 ± 0.1 min) that could be readily quantified on top of the TiO_2 NPs peak (still at 8.6 ± 0.1 min). Thus the chemical method was proven to be capable of identifying SiO_2 NPs and quantifying them with enhanced sensitivity.

Coating of silica and titania nanoparticles with chitosan

Coating of SiO_2 NPs with chitosan was next investigated. A significant increase in hydrodynamic diameter, from 53 ± 3 nm for SiO_2 particles to 513 ± 30 nm for chitosan-coated SiO_2 particles (at 20 g/L) was observed, as shown in table 1. Electrostatic and hydrogen bonding interactions between chitosan amide groups and silanol groups enabled the encapsulation process [26]. The uniform suspension of chitosan-coated SiO_2 particles did not precipitate upon dilution with a 10 mM KNO_3 solution in water during the sample preparation for DLS analysis [27]. Analysis of chitosan-coated SiO_2 particles by CE-UV failed badly because chitosan interacted with the capillary inner wall via electrostatic attraction, reducing the electroosmotic flow (EOF) down to zero. Similarly, coating of TiO_2 NPs with chitosan produced chitosan-coated TiO_2 NPs with a hydrodynamic diameter of 477 ± 11 nm, which is significantly larger than the 155 ± 6 nm for TiO_2 NPs.

HPMA binding with chitosan-coated nanoparticles

Afterwards, the interaction of HPMA with chitosan-coated SiO_2 particles was investigated. Initially the hydrodynamic diameter of the chitosan-coated SiO_2 particles decreased to 417 ± 17 nm. One plausible reason for the reduction in the hydrodynamic diameter of chitosan-coated SiO_2 particles upon HPMA binding is that HPMA disturbed the natural agglomeration tendency of chitosan [28]. The hypothesis is that chitosan initially formed a loose coating (by surface adsorption onto SiO_2 or TiO_2) that condensed upon addition of HPMA. Further addition of HPMA, however, changed the hydrodynamic diameter to 440 ± 12 nm. Similarly, HPMA (at 0.05% v/v) interacted with chitosan-coated TiO_2 NPs decreasing their hydrodynamic diameter from 477 ± 11 nm to 416 ± 11 nm. However, further addition of HPMA (at 0.1% v/v) increased their hydrodynamic diameter to 514 ± 8 nm.

A significant increase in peak area was observed after HPMA (0.03% v/v) bound to chitosan-coated SiO_2 particles. More importantly, after HPMA binding, CE-UV analysis could be performed with no disturbance of the EOF. Figure 4 shows the improved detection of HPMA-bound chitosan-coated SiO_2 particles. Upon varying the SiO_2 concentration in chitosan suspension, the resultant HPMA-bound chitosan-coated SiO_2 peak area changed accordingly as shown in Figure 5. A significant total enhancement of 50 folds in detection sensitivity was attained by coating SiO_2 NPs with chitosan followed by

Particles	Hydrodynamic Diameter (nm)	HPMA Thickness (nm)	Coating Thickness (nm)	Polydispersity Index (PDI)
SiO_2	53 ± 3	---	---	0.357
HPMA-bound SiO_2	83 ± 13	30	---	0.356
TiO_2	155 ± 6	---	---	0.319
HPMA – TiO_2 mixture	154 ± 5	0	---	0.323
Chitosan-coated SiO_2	513 ± 30	---	460	0.343
HPMA-bound chitosan-coated SiO_2 (HPMA at 0.05% to 0.1% v/v)	417 ± 17 to 440 ± 12	-96 to -73	---	0.322-0.338
Chitosan-coated TiO_2 (SDS)	477 ± 11	---	322	0.300
HPMA-bound chitosan-coated TiO_2 (HPMA at 0.05% to 0.1% v/v)	416 ± 11 to 514 ± 8	-61 to +37	---	0.122-0.288

Table 1: DLS analysis to determine the hydrodynamic diameters of different particles, followed by calculation of the HPMA thickness.

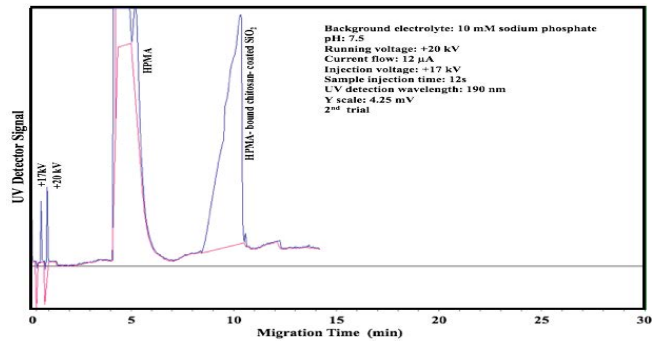

Figure 4: CE-UV characterization of HPMA-bound chitosan-coated SiO_2 particles.

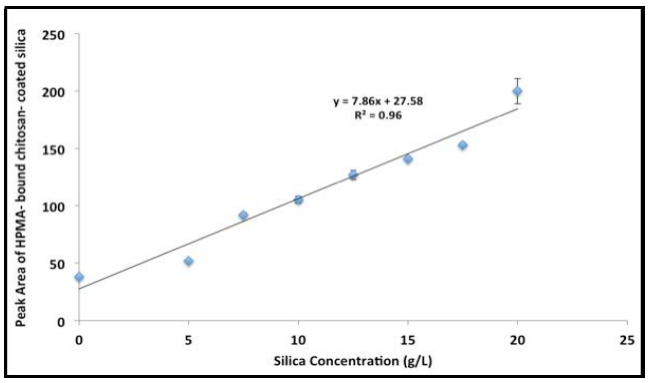

Figure 5: HPMA-bound chitosan-coated SiO_2 peak areas obtained for different SiO_2 concentrations.

HPMA binding. This result is better than the enhancement of 10-14 folds previously attained by using both PHPMA and PDA coatings. In addition, no chemical initiator is needed for this novel technique which does not involve in-situ polymerization.

Similarly, HPMA-bound chitosan-coated TiO_2 NPs were easily analyzed by CE-UV in conjunction with improvement of the CE-UV detection of chitosan-coated TiO_2 NPs as shown. All these results provide clear and convincing proof that SiO_2 NPs can be made larger in size by interaction with HPMA alone and even larger after coating with chitosan under very simple experimental conditions. The larger sizes offer more sensitive detection of SiO_2 NPs in a water sample by CE-UV analysis.

Conclusions

A simple and inexpensive method for the detection of nanoparticles, which are a burden in aquatic ecosystem, has been successfully developed. Hydroxypropyl methacrylate interacted with colloidal SiO_2 nanoparticles to produce a larger size for more sensitive detection by CE-UV. It did not interact with TiO_2 nanoparticles in aqueous suspension, resulting in no change of CE-UV detection sensitivity. It interacted with chitosan-coated SiO_2 or TiO_2 nanoparticles, resulting in a significant enhancement of their CE-UV detection. This chemical technique allows us to analyze an aqueous sample containing different kinds of nanoparticles, both qualitatively and quantitatively, simply by adding hydroxypropyl methacrylate to observe any CE-UV peak enhancements. HPMA interaction is time-saving as less than 22 hours can be used to reach a binding equilibrium with the nanoparticles. Coating of SiO_2 and TiO_2 NPs with chitosan produced a significant increase in hydrodynamic diameter to 513 ± 30 nm for chitosan-coated SiO_2 particles and 477 ± 11 nm for chitosan-coated TiO_2 nanoparticles. Subsequent HPMA binding facilitated CE-UV analysis without causing disturbance of the EOF. A total enhancement of 50 folds in detection sensitivity was attained by coating SiO_2 nanoparticles with chitosan followed by HPMA binding. The new detection limit is estimated at 0.06 g/L of SiO_2. Only nanoparticles, but not organic compounds, would change in area and migration time after binding to HPMA or coating with chitosan. No chemical initiator is required, unlike what we reported previously using in-situ polymerization to attain coating with PHPMA. In our future work, the ligand-directed formation of colloidal polymers through chemical interactions of surface ligands between adjacent nanoparticles [29] can further enhance the CE-UV detection sensitivity of SiO_2, TiO_2, and other kinds of NPs.

Acknowledgements

Financial support from NSERC Canada is gratefully acknowledged. S. Alsudir thanks the Saudi Ministry of Higher Education for her scholarship.

References

1. Pinna A, Lasio B, Carboni D, Marceddu S, Malfatti L, et al. (2014) Engineering the surface of hybrid organic-inorganic films with orthogonal grafting of oxide nanoparticles. J Nanopart Res 16: 2463-2474.
2. Cheng Z, Dai Y, Kang X, Li C, Huang S, et al. (2014) Gelatin-encapsulated iron oxide nanoparticles for platinum (IV) prodrug delivery, enzyme-stimulated release and MRI. Biomaterials 35: 6359-6368.
3. Sarkar A, Ghosh M, Sil PC (2014) Nanotoxicity: oxidative stress mediated toxicity of metal and metal oxide nanoparticles. J Nanosci Nanotechnol 14: 730-743.
4. Gong XQ, Selloni A (2005) Reactivity of anatase TiO(2) nanoparticles: the role of the minority (001) surface. J Phys Chem B 109: 19560-19562.
5. Reidy B, Haase A, Luch A, Dawson KA, Lynch A (2013) Mechanisms of silver nanoparticle release, transformation and toxicity: a critical review of current knowledge and recommendations for future studies and applications. Materials 6: 2295-2350.
6. Klaine SJ, Alvarez PJ, Batley GE, Fernandes TF, Handy RD, et al. (2008) Nanomaterials in the environment: behavior, fate, bioavailability, and effects. Environ Toxicol Chem 27: 1825-1851.

7. Frimmel FH, Niessner R (2010) Nanoparticles in the Water Cycle: Properties, Analysis and Environmental Relevance. Springer, New York
8. Giovanni M, Tay CY, Setyawati MI, Xie J, Ong CN, et al. (2014) Toxicity profiling of water contextual zinc oxide, silver, and titanium dioxide nanoparticles in human oral and gastrointestinal cell systems.Environ Toxicol.
9. Lai JC, Lai MB, Jandhyam S, Dukhande VV, Bhushan A, et al. (2008) Exposure to titanium dioxide and other metallic oxide nanoparticles induces cytotoxicity on human neural cells and fibroblasts. Int J Nanomedicine 3: 533-545.
10. Li J, Chang X, Chen X, Gu Z, Zhao F3, et al. (2014) Toxicity of inorganic nanomaterials in biomedical imaging. Biotechnol Adv 32: 727-743.
11. Mendes RG, Koch B, Bachmatiuk A, El-Gendy AA, Krupskaya Y, et al. (2014) Synthesis and toxicity characterization of carbon coated iron oxide nanoparticles with highly defined size distributions. Biochim Biophys Acta 1840: 160-169.
12. Chang YN, Zhang M, Xia L, Zhang J, Xing G (2012) The toxic effects and mechanisms of CuO and ZnO nanoparticles. Materials 5: 2850-2871.
13. Wehling J, Volkmann E, Grieb T, Rosenauer A, Maas M, et al. (2013) A critical study: assessment of the effect of silica particles from 15 to 500 nm on bacterial viability. Environ Pollut 176: 292-299.
14. Bundschuh T, Yun JI, Knopp R (2001) Determination of size, concentration and elemental composition of colloids with laser-induced breakdown detection/ spectroscopy (LIBD/S). Fresenius J Anal Chem 371: 1063-1069.
15. Diallo MS, Glinka CJ, Goddard WA, Johnson JH (2005) Characterization of nanoparticles and colloids in aquatic systems 1. Small angle neutron scattering investigations of Suwannee River fulvic acid aggregates in aqueous solutions. J Nanoparticle Res 7: 435-448.
16. Kuyper CL, Fujimoto BS, Zhao Y, Schiro PG, Chiu DT (2006) Accurate sizing of nanoparticles using confocal correlation spectroscopy. J Phys Chem B 110: 24433-24441.
17. Ladj R, Bitar A, Eissa MM, Fessi H, Mugnier Y, et al. (2013) Polymer encapsulation of inorganic nanoparticles for biomedical applications. Int J Pharm 458: 230-241.
18. Yamada H, Urata C, Higashitamori S, Aoyama Y, Yamauchi Y et al. (2014). Critical roles of cationic surfactants in the preparation of colloidal mesostructured silica nanoparticles: control of mesostructure, particle size, and dispersion. ACS Appl Mater Interfaces 6: 3491-3500.
19. Zou H, Wu S, Shen J (2008) Polymer/silica nanocomposites: preparation, characterization, properties, and applications. Chem Rev 108: 3893-3957.
20. Moraes J, Ohno K, Maschmeyer T, Perrier S (2013) Synthesis of silica-polymer core-shell nanoparticles by reversible addition-fragmentation chain transfer polymerization. Chem Commun (Camb) 49: 9077-9088.
21. Alsudir S, Lai EPC (2014) Polymer coatings for sensitive analysis of colloidal silica nanoparticles in Water. Colloid Polym Sci 292: 1289-1296.
22. Alsudir S, Iqbal Z, Lai EP (2012) Competitive CE-UV binding tests for selective recognition of bisphenol A by molecularly imprinted polymer particles. Electrophoresis 33: 1255-1262.
23. Shuai HH, Yang CY, Harn HIC, York RL, Liao TC, et al. (2013) Using surfaces to modulate the morphology and structure of attached cells-a case of cancer cells on chitosan membranes. Chem Sci 4: 3058-3067.
24. Reijnders L (2009) The release of TiO_2 and SiO_2 nanoparticles from nanocomposites. Polym Degrad Stab 94: 873-876.
25. Fede C, Selvestrel F, Compagnin C, Mognato M, Mancin F, et al. (2012) The toxicity outcome of silica nanoparticles (Ludox®) is influenced by testing techniques and treatment modalities. Anal Bioanal Chem 404: 1789-1802.
26. Al-Sagheer F, Muslim S (2010) Thermal and mechanical properties of chitosan/ SiO2 hybrid composites. J Nanomater.
27. Farrell E, Brousseau JL (2014) Guide for DLS sample preparation.
28. El-Hefian EA, Nasef MM, Yahaya AH (2014) Chitosan-based polymer blends: current status and applications. J Chem Soc Pak 36: 11-27.
29. Hill LJ, Pinna N, Char K, Pyun J (2015) Colloidal polymers from inorganic nanoparticles monomers. Prog Polym Sci 40: 85-120